RNA (2000), *6*:1174–1184. Cambridge University Press. Printed in the USA.

Mutations in helix 27 of the yeast *Saccharomyces cerevisiae* 18S rRNA affect the function of the decoding center of the ribosome

IRINA V. VELICHUTINA,[1] JOHN DRESIOS,[2] JOO YUN HONG,[1] CHIBO LI,[1] ALEXANDER MANKIN,[3] DENNIS SYNETOS,[2] and SUSAN W. LIEBMAN[1]

[1]Laboratory for Molecular Biology, Department of Biological Sciences, University of Illinois at Chicago, Chicago, Illinois 60607, USA
[2]Laboratory of Biochemistry, School of Medicine, University of Patras, Patras 26110, Greece
[3]Center for Pharmaceutical Biotechnology, University of Illinois, Chicago, Illinois 60607, USA

ABSTRACT

A dynamic structural rearrangement in the phylogenetically conserved helix 27 of *Escherichia coli* 16S rRNA has been proposed to directly affect the accuracy of translational decoding by switching between "accurate" and "error-prone" conformations. To examine the function of helix 27 in eukaryotes, random and site-specific mutations in helix 27 of the yeast *Saccharomyces cerevisiae* 18S rRNA have been characterized. Mutations at positions of yeast 18S rRNA corresponding to *E. coli* 886 (*rdn8*), 888 (*rdn6*), and 912 (*rdn4*) increased translational accuracy in vivo and in vitro, and caused a reduction in tRNA binding to the A-site of mutant ribosomes. The double *rdn4rdn6* mutation separated the killing and stop-codon readthrough effects of the aminoglycoside antibiotic, paromomycin, implicating a direct involvement of yeast helix 27 in accurate recognition of codons by tRNA or release factor eRF1. Although our data in yeast does not support a conformational switch model analogous to that proposed for helix 27 of *E. coli* 16S rRNA, it strongly suggests a functional conservation of this region in tRNA selection.

Keywords: conformational switch; paromomycin; translational accuracy

INTRODUCTION

The accuracy of protein biosynthesis is determined by the ability of the ribosome to discriminate between a complementary (cognate) and mismatched (near-cognate or noncognate) mRNA–tRNA codon–anticodon complex. Although the precise molecular mechanism of the cognate tRNA selection within the aminoacyl–tRNA site (A-site) of the ribosome is not known, a two-step mechanism of tRNA selection has been proposed (Hopfield, 1974). According to this mechanism, the initial tRNA selection is followed by a proofreading step (Ruusala et al., 1982; Thompson et al., 1986). Recent findings provide evidence for an induced-fit mechanism of tRNA selection, suggesting a direct role for the ribosome in the recognition of the codon–anticodon complex during decoding (Pape et al., 1999). Although the molecular basis for this recognition remains unknown, it has been proposed that interaction between rRNA and the codon–anticodon complex is crucial for the accuracy of tRNA selection (VanLoock et al., 1999). Indeed, molecular contacts between universally conserved adenines A1492 and A1493 in the decoding region of *Escherichia coli* 16S rRNA and the backbone of the mRNA codon in the cognate mRNA–tRNA helix appears to be essential for A-site tRNA binding (Yoshizawa et al., 1999). The lack of contact between rRNA and the near-cognate or noncognate codon–anticodon imperfect helixes are proposed to increase the dissociation rate of incorrect tRNA, thus providing a mechanism for the initial step of tRNA discrimination. In contrast, successful codon–anticodon interaction is predicted to trigger conformational changes in the ribosome that lead to rapid GTPase activation followed by the proofreading step, thereby accomplishing accurate decoding.

A link between the accuracy of translational decoding and a conformational rearrangement between two alternative structures ("error-prone" and "accurate") in helix 27 of *E. coli* 16S rRNA has been suggested (Lodmell & Dahlberg, 1997). According to this model, a dynamic equilibrium between the error-prone and accurate conformations is controlled by a molecular switch mech-

Reprint requests to: Dr. S.W. Liebman, University of Illinois at Chicago, Department of Biological Sciences, Molecular Biology Research Building, 900 South Ashland Avenue, Room 4070, Chicago, Illinois 60607, USA; e-mail: suel@uic.edu.

anism. A shift in the equilibrium between two rRNA conformations caused by mutations in helix 27 was proposed to stabilize one or the other conformational state, thereby leading to an increase or decrease of translational errors, respectively. A three-dimensional cryoelectron-micrographic comparison of the structure of *E. coli* 70S ribosomes isolated from one error-prone and one accurate helix 27 rRNA mutant revealed large-scale structural differences that are predicted to reflect functional changes caused by the shift to the error-prone or accurate conformational state (Gabashvili et al., 1999). Recent X-ray analysis of the *Thermus thermophilus* 30S ribosomal subunit and 70S ribosome (Cate et al., 1999; Clemons et al., 1999) revealed that helix 27 makes extensive minor-groove contacts with the penultimate stem, helix 44, near the decoding site where the A-site tRNA binds to the ribosome. This suggests that helix 27 may influence translational accuracy by affecting the conformation of the decoding region. In addition, nt 909 of helix 27 and nt 1413 and 1487 of helix 44 are protected from chemical attack by antibiotics that increase the error frequency of translation (Moazed & Noller, 1987). The same nucleotides are also protected by either tRNA or the 50S subunit (Moazed & Noller, 1986; Merryman et al., 1999), thus implicating helix 27 together with helix 44 in tRNA binding, subunit association, and translational accuracy. Helix 27 has been also implicated in translocation, because mutations in this region in *E. coli* induce translational frameshifting and cause sensitivity to spectinomycin, an inhibitor EF-G-dependent translocation (Lodmell & Dahlberg, 1997).

One successful genetic approach to study mechanisms of translational decoding is to isolate suppressor and antisuppressor mutations that increase or decrease translational misreading, respectively. Using this approach, several ribosomal proteins and translational factors have been implicated in the control of translational fidelity and/or termination in both prokaryotes and eukaryotes (Vijgenboom et al., 1985; Kawakami & Nakamura, 1990; Hinnebusch & Liebman, 1991; Kraal et al., 1995; Liebman et al., 1995; Mugnier & Tuite, 1999). Mutations in highly conserved domains of small and large ribosomal RNAs have also been found to affect translational accuracy, providing important clues for the role rRNA plays in the decoding process (Chernoff et al., 1994, 1996; Liu & Liebman, 1996; O'Connor et al., 1997; Pagel et al., 1997; Arkov et al., 1998).

The majority of information connecting rRNA to translational fidelity comes from prokaryotic systems. To explore the functional role of eukaryotic rRNAs in translational accuracy, we examined the effect of mutations in helix 27 of yeast *Saccharomyces cerevisiae* 18S rRNA (Fig. 1). A plasmid exchange system (Chernoff et al., 1994) where wild-type rDNA is entirely replaced with the plasmid-borne mutant rDNA was employed.

Here we show that as in *E. coli*, mutations in helix 27 of *S. cerevisiae* 18S rRNA affect translational fidelity. However, the phenotypes of these mutations contradict the expectations of the conformational switch model suggested for *E. coli* 16S rRNA. In addition, we describe a mutation in helix 27 that abolishes the ability of paromomycin to promote the readthrough of stop codons but that remains sensitive to the killing effect of the drug.

RESULTS

The G886A change in the 18S rRNA gene decreases readthrough at stop codons

A genetic screen for random antisuppressor mutations in rRNAs was performed using strain L1524, which contains a mutation in the *SUP45* gene coding for translational termination factor 1, eRF1. The *sup45* mutation results in translational readthrough (suppression) of premature stop codons in the *ade1-14*$_{UGA}$ and *his7-1*$_{UAA}$ mRNAs, thereby allowing *sup45*-mutant cells to grow on media lacking adenine or histidine (Fig. 2A). Accordingly, the inhibition of *sup45*-mediated nonsense suppression caused by antisuppressor mutations in the rRNA genes can be monitored readily as a selective growth inhibition on synthetic media lacking adenine or histidine, without any growth inhibition on synthetic complete media.

The rDNA plasmid (see Materials and methods; Table 1) containing coding regions for all rRNAs as well as the *TRP1 LEU2d* genes (pRDN-wt-TL) was mutagenized with hydroxylamine in vitro, followed by transformation into L1524, bearing a stable deletion of the rDNA repeats on the chromosome and a wild-type rDNA locus on a multicopy *URA3*-plasmid, pRDN-wt-U. About 5,000 Trp$^+$ transformants were patched on −Leu medium to select for cells in which the mutagenized pRDN-TL plasmid is amplified. Following incubation on −Leu medium, cells were transferred to −Ade −Leu and −His−Leu media to score for the efficiency of nonsense suppression. One mutant, *rdn8*, was found to inhibit *sup45*-mediated readthrough of nonsense codons. The level of inhibition of the *ade1-14*$_{UGA}$ readthrough in the *rdn8* mutant was also seen as a color difference on YPD medium: the darker the color, the stronger the inhibition of *sup45*-mediated readthrough (data not shown). The same phenotype was observed in this mutant after complete loss of host pRDN-wt-U plasmid on medium containing 5-fluoroorotic acid (5-FOA; see Materials and methods). Plasmid isolated from the *rdn8* mutant cells was reintroduced into L1524, and resultant transformants were found to inhibit *sup45*-mediated nonsense suppression, thereby confirming plasmid-associated antisuppression.

Using a DNA fragment exchange technique, the *rdn8* mutation was mapped to helix 27 of the 18S rRNA

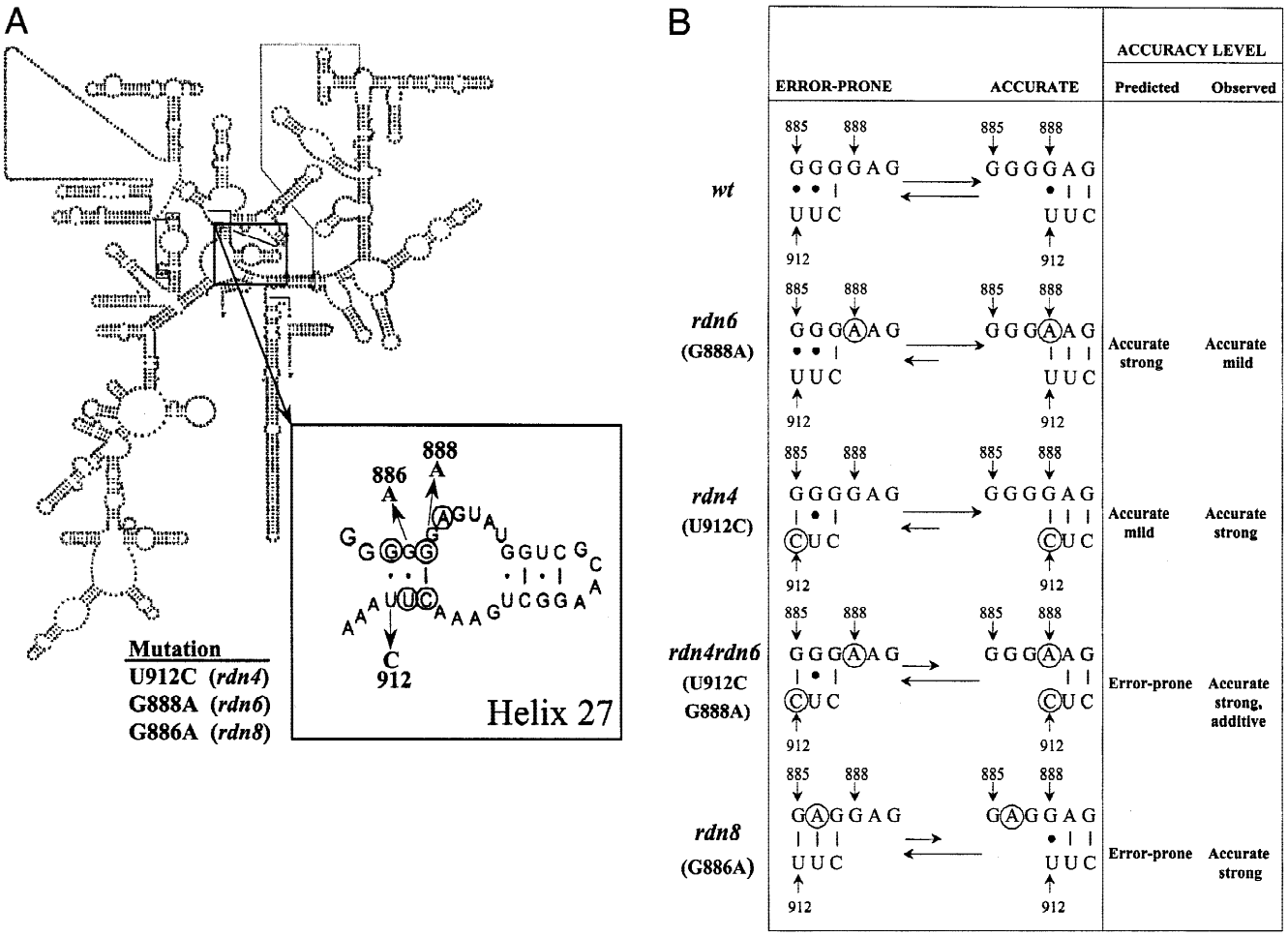

FIGURE 1. Yeast helix 27 mutations tested in the *E. coli* conformational switch model. **A**: The secondary structure of *Saccharomyces cerevisiae* 18S rRNA using position numbers corresponding to *E. coli* 16S rRNA. The secondary structure of helix 27 is shown as predicted by comparative rRNA analysis (Gutell et al., 1994; R. Gutell, http://www.rna.icmb.utexas.edu/). Phylogenetically conserved nucleotides (>95% conservation among three phylogenetic domains including chloroplasts and mitochondria) are circled. The positions of mutations are indicated by arrows. **B**: Mutations in helix 27 of yeast 18S rRNA that are predicted to alter the equilibrium between two alternative structures, 912–910/885–887 and 912–910/888–890. The proposed stabilization of one structure was predicted in the *rdn* mutants relative to the wild-type using the *mfold 3.0* program (Zuker & Jacobson, 1998; Mathews et al., 1999) and is indicated by the longer arrow. Mutations are shown in circles. According to the conformational switch model (Lodmell & Dahlberg, 1997), stabilization of the 912–910/885–887 structure is predicted to result in an increased level of translational errors (error-prone). Stabilization of the alternative 912–910/888–890 structure is proposed to decrease the level of translational misreading (accurate). The translational accuracy phenotypes predicted by this model and those observed for the different yeast *rdn* mutants are listed.

gene (Mueller & Brimacombe, 1997). DNA sequence analysis of the *Sac*I-*Sac*II DNA fragment revealed a unique G → A change at position 886 of the highly conserved helix 27 of the small ribosomal RNA (Fig. 1).

Mutations that stabilize or destabilize the base-pairing potential of positions 912 and 888 decrease readthrough of stop codons

The conformational switch model predicts that the *rdn8* alteration should decrease translational fidelity, because the G886A change strengthens the 886–911 base pair of the 912–910/885–887 error-prone structure in helix 27 (Lodmell & Dahlberg, 1997; Fig. 1B). Unexpectedly, we found that *rdn8* decreases translational readthrough of stop codons. To examine whether changes in the stability of the alternative 912–910/888–890 accurate helix would affect translational fidelity as predicted by the model, mutations that either stabilize or destabilize 912–888 base pairing were introduced into helix 27 by site-directed mutagenesis. The effect of these changes on translational accuracy was characterized both in vivo and in vitro.

We introduced G888A (*rdn6*) that replaces a wobble U912-G888 pair with the canonical U912-A888 pair into pRDN-TL plasmid, creating pRDN-*rdn6*-TL. Following transformation of pRDN-*rdn6*-TL into L1524, cells that lost pRDN-wt-U host plasmid and kept pRDN-*rdn6*-TL

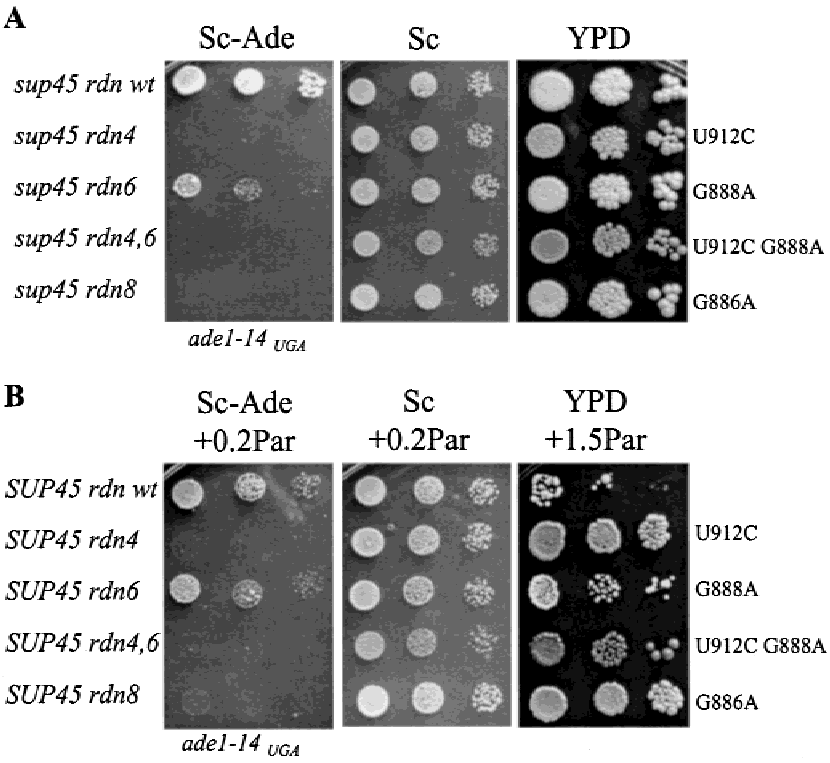

FIGURE 2. Mutations in helix 27 of the 18S rRNA increase translational accuracy during stop-codon decoding. The rDNA mutations inhibit readthrough of the *ade1-14*$_{UGA}$ nonsense codon, mediated by (**A**) *sup45* mutation in L1524 (*sup45 rdn wt*) or by (**B**) paromomycin (0.2 mg/mL in synthetic media or 1.5 mg/mL in YPD) in L1521 (*rdn wt*). Wild-type, pRDN-wt-TL, and mutant pRDN-*rdn4*-TL, pRDN-*rdn6*-TL, pRDN-*rdn4rdn6*-TL, and pRDN-*rdn8*-TL plasmids were introduced into L1524(pRDN-wt-U) and L1521(pRDN-wt-U) strains, followed by loss of the host pRDN-wt-U plasmid on +FOA medium. The level of cell growth on Sc-Ade and −Ade+0.2 Par media is indicative of the stop-codon readthrough efficiency, mediated by the *sup45* mutation and paromomycin, respectively. The level of inhibition of the *ade1-14*$_{UGA}$ readthrough induced by paromomycin is seen as a shading difference on YPD+Par (1.5 mg/mL): the darker the shading, the stronger the inhibition of paromomycin-mediated readthrough. Translational accuracy during stop-codon decoding was tested by comparing the growth of 10-fold serial dilutions of yeast strains carrying either the wild-type or mutant 18S rRNA gene spotted on the indicated media and incubated at 30 °C for 5 days.

were selected. As shown in Figure 2A, the G888A change results in inhibition of *sup45*-induced nonsense suppression, monitored as reduced growth on −Ade medium compared to the L1524 strain carrying wild-type rDNA. The *rdn6*-mediated antisuppression effect is much weaker than that previously described for the *rdn4* (U912C) mutation (Chernoff et al., 1994), which stabilized the 912–888 base pair to a higher degree (Fig. 2A). The "accuracy" phenotypes of these two mutants, *rdn4* and *rdn6*, are consistent with the prediction of the switch model.

Next we asked if a combination of the *rdn4* and *rdn6* mutations would reverse the accuracy phenotypes of the single mutants, as predicted by the model. The *rdn4rdn6* double mutant is predicted to have the reverse phenotype from the single mutants (Fig. 1B) because in the double mutant the 912–888 base pair is destabilized (C912*A888 mismatch in the *rdn4rdn6* versus wobble U912•G888 base pair in wild-type rRNA), whereas the 912–885 base pair is enhanced (canonical C912–G885 base pair in the *rdn4rdn6* versus wobble U912•G888 base pair in wild-type rRNA). Contrary to the prediction, when the rDNA of wild-type for *SUP45* strain L1521 was replaced with rDNA encoding the *rdn4rdn6* double mutation, the strain failed to grow on −Ade and −His media, showing no increase in translational readthrough of the *ade1-14*$_{UGA}$ and *his7-1*$_{UAA}$ nonsense codons (data not shown). Rather, the *rdn4rdn6*-mutant cells exhibited an inhibition of *sup45*-mediated nonsense suppression that is stronger than exhibited by either of the single mutants (Fig. 2A).

TABLE 1. pRDN plasmids.

Name	rRNA	Plasmid markers
pRDN-wt-TL	wild-type	*TRP1 LEU2-d*
pRDN-*rdn4*-TL	U912C	*TRP1 LEU2-d*
pRDN-*rdn6*-TL	G888A	*TRP1 LEU2-d*
pRDN-*rdn4rdn6*-TL	U912C G888A	*TRP1 LEU2-d*
pRDN-*rdn8*-TL	G886A	*TRP1 LEU2-d*

Mutations in helix 27 of yeast 18S rRNA inhibit nonsense suppression caused by paromomycin

In previous sections we described the isolation of rRNA mutations that inhibit readthrough of stop codons caused by a mutation in release factor 1, *sup45*. Here we ask whether the isolated rRNA mutations would inhibit stop-codon readthrough induced by paromomycin. Paromomycin is an aminoglycoside antibiotic known to directly bind to the A-site of *E. coli* 16S rRNA and interfere with translational decoding, inducing misreading (Fourmy et al., 1998; Puglisi et al., 2000). The drug also causes translational misreading in yeast (Palmer et al., 1979).

A *SUP45* wild-type rDNA deletion strain, carrying either wild-type (pRDN-wt-TL) or *rdn*-mutant (pRDN-

rdn4-TL, pRDN-*rdn6*-TL, pRDN-*rdn4rdn6*-TL, pRDN-*rdn8*-TL) plasmids was tested for the ability to grow on −Ade medium in the presence of low levels of paromomycin (0.2 mg/mL). As shown in Figure 2B, a strain bearing wild-type rDNA grows on medium lacking adenine in the presence of paromomycin and is white on YPD/paromomycin medium, indicative of efficient paromomycin-induced readthrough of the *ade1-14*$_{UGA}$ nonsense allele. No growth on −Ade medium was observed in the absence of paromomycin (data not shown). In contrast, single *rdn4*, *rdn8*, and double *rdn4rdn6* mutants inhibit paromomycin-mediated stop-codon readthrough. The antisuppression effect of the *rdn6* toward paromomycin, however, is much weaker, which is consistent with a mild inhibition of the *sup45*-mediated suppression caused by *rdn6* mutation (Fig. 2A). The *rdn4rdn6* double mutant exhibits the strongest antisuppression toward paromomycin indicated by intense red color on YPD medium in the presence of 1.5 mg/mL paromomycin. The *rdn4rdn6*-mediated antisuppression cannot be explained by the inability of paromomycin to bind to the mutant ribosomes, because the *rdn4rdn6* double mutant is at least 10-fold more sensitive to the killing effect of 1.5 mg/mL paromomycin than the single *rdn4* mutant, in which some paromomycin-mediated stop-codon readthrough is still observed (Fig. 2B, see shading differences).

Effect of *rdn* mutations on translational accuracy in vitro

To examine whether the mutations in helix 27 specifically affect readthrough at stop codons or increase the accuracy of decoding at sense codons as well, we measured the misincorporation of the near-cognate amino acid leucine relative to the cognate amino acid phenylalanine using a poly(U)-dependent cell-free translational system. As shown in Table 2, the presence of each of the *rdn* mutations caused a decrease of the translational error frequency, showing that, as predicted by the in vivo results, all the rRNA mutations under study increase the accuracy of decoding. The strongest effect was exhibited by the double *rdn4rdn6* mutation, which decreased translational errors almost threefold. Importantly, the accuracy phenotype of the double *rdn4rdn6* mutant tested in vitro was additive, which is in good agreement with the accuracy phenotype found in vivo.

The effect of the rRNA mutations on accuracy correlated with the reduced affinity of tRNA for the A-sites of mutant ribosomes (Fig. 3) exhibiting the most impaired binding for the *rdn4rdn6*-mutant ribosomes. In addition, the double *rdn4rdn6* mutant shows decreased binding of tRNA to the ribosomal P-site, which can explain the observed decrease in the activity of polyphenylalanine synthesis measured in vitro (Table 2).

TABLE 2. Efficiency of polyphenylalanine synthesis and translational error frequencies measured in cell-free system.

Ribosome type[a]	PolyPhe activity (pmol Phe/pmol Rib)	Error frequency ± S.D.
rdn wt	14	0.0166 ± 0.0023
rdn4	14	0.0098 ± 0.0010
rdn6	14	0.0121 ± 0.0014
rdn4rdn6	9	0.0057 ± 0.0009
rdn8	14	0.0118 ± 0.0019

[a]Ribosomes were isolated from isogenic derivatives of *sup45*-mutant strain L1524.

Chemical probing of ribosomal RNA structure

Kethoxal, which specifically modifies guanines not involved in a Watson–Crick base pair, was used to test whether the rRNA mutations affect the conformation of helix 27. The relative efficiency of modifying guanines at positions 885, 886, 887, and 890 was compared between wild-type, *rdn4*, *rdn6*, *rdn4rdn6,* and *rdn8* ribosomes using the primer extension method (Stern et al., 1986), but no notable differences in the reactivity of helix 27 nucleotides were found (Fig. 4), suggesting that neither stabilization nor destabilization of the 912–888 base pair influenced the overall structure of this helix.

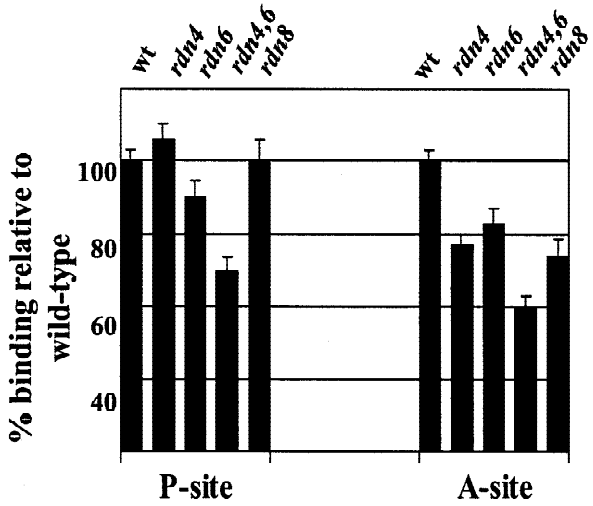

FIGURE 3. Efficiency of tRNA binding to the P- and A-site of the ribosome. The P- and A-site binding capacities of the mutant ribosomes are expressed as percent of the P- and A-site binding capacities of the wild-type ribosomes. The P-site binding was measured as the amount of {N-Ac-[^{3}H]Phe-tRNA^{Phe}•80S•poly(U)} complex immobilized on cellulose nitrate filters under conditions described in Materials and methods. The A-site binding was measured as the amount of [^{3}H]Phe-tRNA^{Phe}•80S•poly(U) complex immobilized on cellulose nitrate filters after the P-site was completely filled with an excess of tRNA^{Phe}.

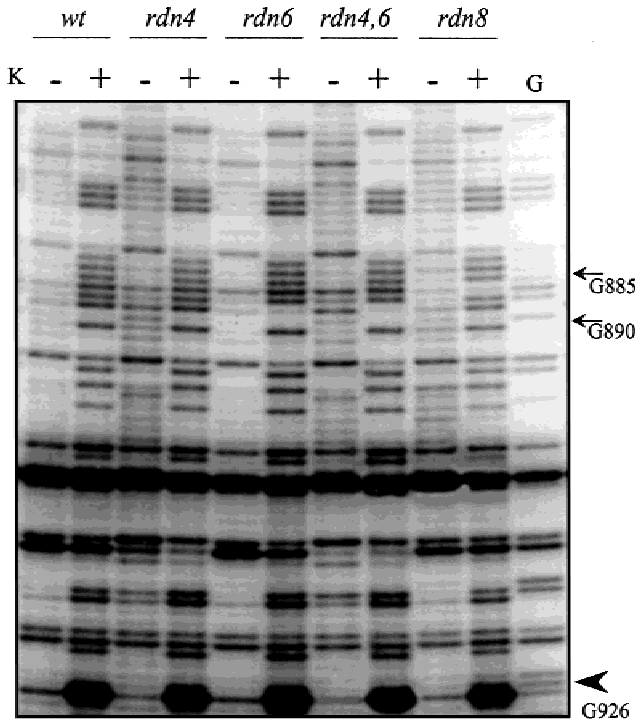

FIGURE 4. Chemical probing of helix 27 of 18S rRNA using kethoxal (K). Ribosomal particles isolated from *sup45* cells containing ether wild-type or mutant (*rdn4, rdn6, rdn4rdn6, rdn8*) 18S rRNA were probed with kethoxal (+). Unmodified ribosomes (−) were used as a control. Following rRNA extraction, modified bases were monitored by primer extension. Positions of nucleotides whose relative accessibility to kethoxal was compared are shown by arrows. The G926 arrowhead points to the nucleotide known to be protected from modification by tRNA bound to the P-site of the *E. coli* ribosome. Nucleotide positions correspond to *E. coli* 16S rRNA numbering. Lane G is the product of dideoxy sequencing of the 18S rRNA.

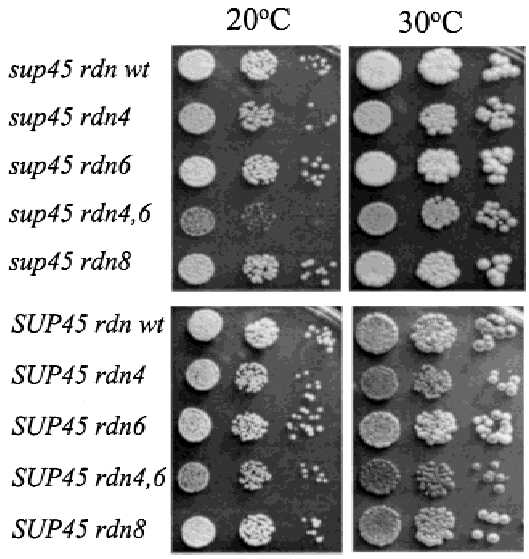

FIGURE 5. Double *rdn4rdn6* mutation causes cold sensitivity in *sup45* mutant cells. Cold sensitivity was scored by spotting 10-fold serial dilutions of *sup45* mutant or *SUP45* wild-type yeast cells bearing either wild-type or *rdn4*, *rdn6, rdn4rdn6*, *rdn8* mutant RDN on YPD medium followed by incubation at 20 °C or 30 °C.

The double *rdn4rdn6* mutation inhibits cell growth and causes an imbalance in ribosomal subunits

Neither *rdn4* nor *rdn6* single mutations affected the growth of yeast cells bearing a *sup45* mutation at either 20 °C or 30 °C (Fig. 5). In contrast, the *rdn4rdn6* double inhibits growth of *sup45* mutant cells but not of wild-type *SUP45* cells. The deleterious effect of the double *rdn4rdn6* mutation was more apparent at 20 °C than at 30 °C.

To gain insight into the effect of the *rdn4rdn6* double mutation on the cell growth, polysome profiles of mutant and wild-type strains were compared (Fig. 6). The polysome profile of a strain carrying a *sup45* mutation and wild-type for rRNA is similar to that of the isogenic *SUP45* wild-type strain. Interestingly, although polysome profiles of *sup45/rdn4* and *sup45/rdn6* single rRNA mutant strains are similar to the polysome contour of the isogenic rRNA wild-type strain, a dramatic increase in the 60S/40S subunit ratio was observed in the *sup45/rdn4rdn6* double rRNA mutant. In contrast, only a minor deficit in the 40S subunit is detected in an *rdn4rdn6* strain that is wild-type for *SUP45*. Thus, the polysome profile data suggests that the small ribosomal subunit assembly or stability is compromised by the *rdn4rdn6* double mutation in *sup45*-mutant but not in *SUP45* wild-type cells. The polysome profile from the *sup45rdn8* strain also shows subunit imbalance, but to a much lesser extent.

DISCUSSION

As established in prokaryotic systems, here we demonstrate that mutations in the homologous helix 27 of yeast *S. cerevisiae* 18S rRNA alter the accuracy of translational decoding. Based on genetic data obtained in *E. coli*, helix 27 was proposed to modulate the accuracy of decoding through a conformational switch between two alternative structures, formed by either 912–910/885–887 or 912–910/888–890 base pairing, that affect accuracy in opposite ways by either increasing or reducing the level of translational errors, respectively (Lodmell & Dahlberg, 1997; Fig. 1B). Our finding that the G886A change caused a strong increase in translational accuracy while stabilizing the predicted 912–910/885–887 error-prone structure, seemingly contradicted the conformational switch model (Table 2, Fig. 1B). We therefore asked if mutations that enhance or destabilize the proposed 912–910/888–890 structure would exert opposite effects on translational accuracy as expected from the model. We found, however, that mutations that stabilize or destabilize the 912–888 base pair all cause an increase in accuracy. According to the switch model, the individual U912C and G888A

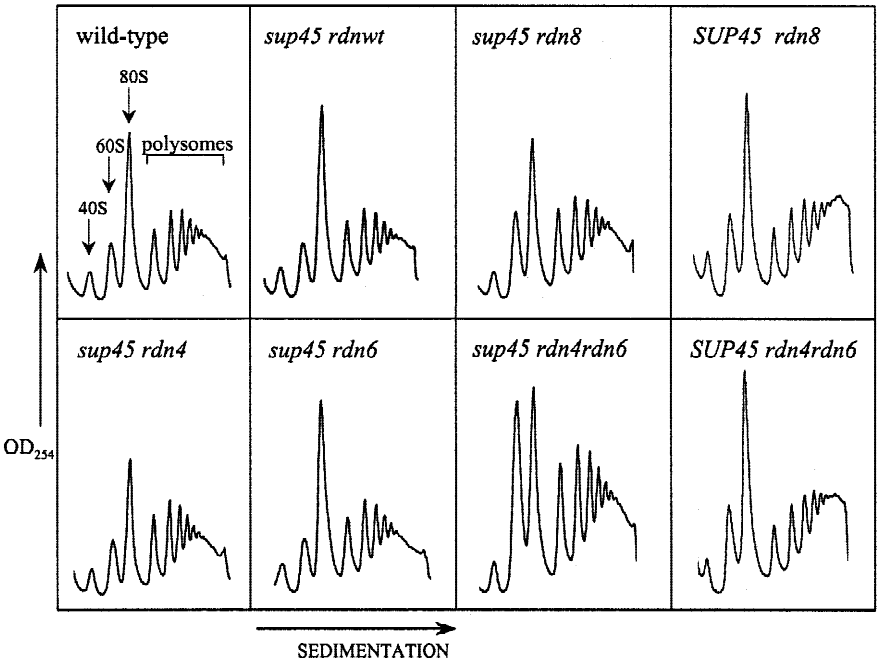

FIGURE 6. A combination of the *rdn4rdn6* and *sup45* mutations results in 60S/40S ribosomal subunit imbalance. Polysomes were extracted from isogenic *SUP45* wild-type or *sup45*-mutant strains (L1521 and L1524, respectively) bearing either wild-type (pRDN-wt-TL) or *rdn*-mutant (pRDN-*rdn4*-TL, pRDN-*rdn6*-TL, pRDN-*rdn4rdn6*-TL, or pRDN-*rdn8*-TL) plasmids. Polysome-containing lysates were prepared from cell cultures grown at 30 °C and were applied to a 10–50% (w/v) sucrose density gradient. Peaks representing free 40S, 60S ribosomal subunits, and 80S monoribosomal and polysomal fractions are labeled.

mutations should make the ribosomes more accurate, whereas their combination should make the ribosome less accurate. In fact we found that either the individual or double mutants make the ribosome more accurate (Table 2; Fig. 1B). Thus in general, the genetic data reported here in yeast do not support the conformational switch model in the control of translational accuracy.

It is worth noting that the conformational switch in helix 27 of *E. coli* ribosome can be modulated by ribosomal proteins S5 and S12, which are shown to protect bases of helix 27 during ribosome assembly (Stern et al., 1989). The observation that mutations in S5 and S12 affect translational fidelity supports this notion. Thus, a failure of yeast helix 27 mutations to follow predictions of the *E. coli* switch model could reflect structural and functional differences in the decoding center of the eukaryotic ribosome. Indeed, although mutations in yeast homologs to *E. coli* S12, S4, and S5 ribosomal proteins have been shown to affect the efficiency of nonsense suppression as in *E. coli*, significant differences do exist between the primary structures of the prokaryotic and eukaryotic proteins. In addition, identical changes in prokaryotic and eukaryotic rRNA can exhibit opposite effects on translational accuracy (O'Connor et al., 1992), suggesting that direct extrapolations from prokaryotes to eukaryotes are difficult. Finally, recent evidence suggests that the structures of bacterial and eukaryotic release factors are significantly different (Song et al., 2000).

Although the requirement for the 912–910/885–887 pairing was demonstrated by compensatory mutations as well as by comparative and structural analysis (Lodmell et al., 1995; Cate et al., 1999), no such analysis suggests that the 912–910/888–890 structure is conserved and essential for viability. Our finding that U912C and G886A mutations increase translational accuracy provides a correlation between the stabilization of the 912–910/885–887 structure and an increase in translational fidelity. The exclusive formation of the 912–910/885–887 structure is consistent with our failure to identify any conformational differences in rRNA structure of the 888–890 region of helix 27 between wild-type and rRNA-mutants.

However, the growth rate and paromomycin-induced readthrough phenotypes we find are consistent with the hypothesis that the U912C and G888A mutations do interact (see below). Likewise, mutations at the 912 and 888 positions of *E. coli* 16S rRNA result in synthetic cell lethality, suggesting an interaction between bases at these positions (Lodmell & Dahlberg, 1997). Our finding that the U912C G888A double mutation causes a deleterious effect on cell growth and a 60S/40S subunit imbalance in the presence of a mutation in termination factor eRF1 (*sup45*), but not in the isogenic strain carrying a wild-type termination factor (Figs. 5 and 6), suggests an interaction between eRF1 and helix 27 of the 18S rRNA. One possible explanation is that eRF1 may be directly involved in rRNA maturation, and the ability of eRF1 to associate with rRNA may be an essential prerequisite for efficient ribosome biogenesis. Alternatively, severely impaired stop-codon recognition caused by both altered eRF1 and the U912C G888A antisuppressor mutations may cause a deficit of a protein that is essential for ribosome biogenesis.

The double U912C G888A rRNA mutation abrogates the ability of paromomycin to induce stop-codon readthrough. Because the U912C G888A double mutant

shows a stronger antisuppression effect toward paromomycin than the single U912C mutant, it was unexpected to find that the U912C G888A double mutant was more sensitive to the drug than the U912C mutant (Fig. 2B). This finding suggests that the U912C G888A double mutation separates the killing and stop-codon readthrough effects of paromomycin. In contrast, although growth of the single U912C mutant is not inhibited by a high concentration of paromomycin, the drug is still able to cause readthrough as indicated by the appearance of a light pink color on complete medium. Because paromomycin is predicted to interfere directly with translational decoding by binding to helix 44 of the small rRNA, near the decoding site (Puglisi et al., 2000), we propose that ribosomes bearing the U912C G888A double mutation are deficient in codon–anticodon recognition. Consistent with this prediction, the U912C G888A mutant ribosomes display a strong decrease in tRNA binding to the A-site of the ribosome (Fig. 3).

Another mechanism by which stop-codon readthrough can be enhanced is to directly increase efficiency of the release factors in termination. Mutations in rRNA that directly enhance the efficiency of termination would be expected to "antisuppress" tRNA suppressor mutations with anticodons complementary to stop codons. However, although the U912C G888A and other helix 27 mutations inhibit stop-codon readthrough caused by mutant eRF1, they failed to enhance termination efficiency of wild-type eRF1 in the presence of stop-codon-specific tRNA (data not shown). This observation, together with the finding that helix 27 mutant ribosomes inhibit misreading of poly-U message in vitro (Table 2; Fig. 3), makes us favor the hypothesis that the rRNA mutations are deficient in codon–anticodon recognition over the possibility of a direct effect of helix 27 mutations on termination.

Alternatively, the involvement of the helix 27 in translocation, rather than in the decoding could explain the inability of paromomycin to cause readthrough in the double mutant. Possibly, in translocation defective ribosomes, the ability of paromomycin to promote tRNA misincorporation is masked by a delay in the ribosome's return to the pretranslocation (paromomycin-competent) state after translocation. Indeed, an rRNA-based mechanism of translocation where a three-base conformational switch in helix 27 defines different tRNA binding states during translocation has been proposed (Wilson & Noller, 1998).

The mechanism of how aminoglycoside antibiotics kill cells remains obscure. Certainly, a general decrease in translational accuracy mediated by aminoglycosides may affect the overall fitness of an organism, as demonstrated for mutants with decreased translational fidelity (Kurland, 1992). On the other hand, it is unclear whether aminoglycosides affect cell viability by interfering with other steps of protein biosynthesis. Our finding that the U912C G888A mutation abolishes the ability of paromomycin to induce readthrough while retaining the ability to cause killing provides an essential genetic tool to explore the exact molecular mechanism of the lethal effect of this clinically important drug.

MATERIALS AND METHODS

Plasmids

The 2-μm high-copy pRDN plasmids used in this study (Table 1) carry the entire 9-kb (wild-type or mutant) rDNA repeat, containing coding regions for both 18S, 25S, 5.8S, and 5S rRNAs under the control of PolI and PolIII promoters, respectively. The *LEU2-d*, promoter-deficient version of the *LEU2* gene is used to select on −Leu medium for yeast cells with high plasmid copy number (Parent et al., 1985). The pRDN-*rdn4*-TL and pRDN-*rdn6*-TL plasmids contain U912C and G888A mutations in the 18S rRNA gene, respectively (Chernoff et al., 1994; Liebman et al., 1995).

pRDN-*rdn4rdn6*-TL bears the double U912C G888A mutation in the 18S rRNA gene, introduced by side-directed mutagenesis using a modification of the overlap extension PCR (Ito et al., 1991). Primer pairs 153/155 (5′-AGCGGA TAACAATTTCACACAGGA-3′ and 5′-C***CTGCCG***GTCGAC TCTAGCGCGCAA-3′, respectively) and 154/*rdn4rdn6*(5′-CGCCAGGGTTTTCCCAGTCACGAC-3′ and 5′-TTT**G**AGT TTCAGCCTTGCGACCATACT**T**CCCC-3′, respectively) were designed to introduce the *rdn4rdn6* double mutation (bold underlined nucleotides) into the gene coding for 18S rRNA. In the second PCR step, overlapping DNA fragments obtained in the first PCR reaction were combined and extended in the presence of primers 153 and 154 to yield a mixture of the mutant *rdn4rdn6* and wild-type rRDN sequences with and without the *Pst*I site (bold italic nucleotides), respectively. The use of the *Pst*I site for subsequent cloning eliminates wild-type rDNA sequence from the final construct. Following PCR, the rDNA product was digested with *Pst*I/*Eco*RI and cloned in the corresponding unique sites in pUC19. The *Sac*I/*Sac*II fragment containing the *rdn4rdn6* double mutation was isolated from the recombinant plasmid and cloned into pRDN-wt-TL, producing pRDN-*rdn4rdn6*-TL. The sequence of the *Sac*I/*Sac*II DNA fragment of the pRDN-*rdn4rdn6*-TL was verified by DNA sequence analysis.

pRDN-*rdn8*-TL carries the *rdn8* mutation in the 18S rRNA, which was isolated in a genetic screen as a mutation that inhibits *sup45*-mediated suppression of *ade1-14*$_{UGA}$ and *his7-1*$_{UAA}$ nonsense alleles. Hydroxylamine mutagenesis of the pRDN-wt-TL plasmid was carried out as described (Rose, 1990).

Strains and cultivation conditions

Yeast strains used in this study are isogenic to strain L1521 (*MAT*a {psi$^-$} *ade1-14*$_{UGA}$ *his7-1*$_{UAA}$ *lys2-L864*$_{UAG}$ *trp1*Δ *ura3-52 leu2-3,112 rdn*Δ,[pRDN-wt-U]). L1521 bears a stable deletion of all chromosomal rDNA repeats and a resident high-copy wild-type rDNA-*URA3* plasmid, pRDN-wt-U, that supports cell viability. Strain L1524 carries an additional mutation in release factor (eRF1), *sup45*, that results in efficient suppression of *ade1-14*$_{UGA}$ and *his7-1*$_{UAA}$ (Chernoff et al., 1996).

Initially, either wild-type (pRDN-wt-TL) or mutant (pRDN-*rdn4*-TL, pRDN-*rdn6*-TL, pRDN-*rdn4rdn6*-TL, and pRDN-*rdn8*-TL) plasmids were introduced into L1521 or L1524 yeast strains, and transformants were obtained on −Trp medium, followed by transfer to −Leu medium to select for cells with amplified pRDN-TL plasmid. Following incubation on −Leu, transformants were replica plated on medium containing FOA (+FOA), selective for Ura$^-$ cells that lost the resident pRDN-wt-U plasmid (plasmid exchange). The resulting colonies are dependent upon the *TRP1 LEU2d*, pRDN-TL plasmid for viability.

RT-PCR products synthesized from ribosomal RNA isolated from wild-type L1521(*SUP45*) or mutant L1524(*sup45*) cells bearing either wild-type (pRDN-wt-TL) or mutant (pRDN-*rdn4*-TL, pRDN-*rdn6*-TL, pRDN-*rdn4rdn6*-TL, pRDN-*rdn8*-TL) plasmids were sequenced to verify the presence of the mutations in the rRNA (data not shown).

Standard yeast (Rose, 1990) and bacterial (Sambrook et al., 1989) media as well as cultivation procedures were used. Yeast transformation was accomplished using the lithium–acetate method (Ito et al., 1983). Synthetic complete (Sc) medium lacking nutrient(s) (e.g., −Trp, −Leu, −Ade, −His) was used to select for transformants or to score for nonsense suppression. Incubation on +FOA medium containing 1 mg/mL 5-FOA and 12 mg/mL of uracil was used to select for Ura$^-$ colonies (Boeke et al., 1984). Organic complete medium (YPD) was used to grow yeast cells at different temperatures. Paromomycin, unless specifically mentioned, was added to YPD medium.

Ribosome isolation and chemical probing

Yeast ribosomes were prepared as described (Grant et al., 1974) with some modifications. Cell cultures were grown at 30 °C to early log phase. Sodium azide (1 mM NaN_3) was added to the culture 15 min before the harvest. Cell pellets were washed with water and resuspended in 1 mL of buffer A (10 mM $MgCl_2$, 100 mM KCl, 50 mM Tris/HCl, pH 7.5, 0.4 μM PMSF) at 4 °C. An equal volume of glass beads (400 μm in diameter; Sigma Chemical Co.) was added and cells were broken by 10–15 pulses of vortexing (15 s each), punctuated with cooling on ice. Cell debris was precipitated at 27,000 × *g* for 15 min (4 °C) and lysate was clarified by centrifugation at 30,000 × *g* for 20 min (4 °C). The ribosomes were pelleted from the supernatant at 160,000 × *g* in a Beckman SW41 rotor for 90 min, resuspended in buffer B (2 mM magnesium acetate, 100 mM potassium acetate, 20 mM HEPES, pH 7.4, 0.1 mM PMSF, 1 mM dithiothreitol (DTT), 20% glycerol) and frozen at −70 °C.

For chemical probing, ribosomes (10 pmol) were preincubated for 5 min at 42 °C in 500 μL of reaction buffer (80 mM potassium cacodylate, pH 7.2, 20 mM $MgCl_2$, 100 mM NH_4Cl). Kethoxal (20 μL, 1:10 (v/v) dilution in ethanol) was added and incubation was continued for 10 min at 37 °C. The reaction was stopped by the addition of 55 μL stop buffer (3 M sodium acetate, 750 mM potassium borate, pH 6.5) followed by the addition of 1 mL cold ethanol. Ribosomes were precipitated; ribosomal RNA was extracted and analyzed by primer extension with the primer s965.rev: 5′-GGTGAGT TTCCCCGTGTTGAG-3′ as described (Stern et al., 1986).

Polyribosome preparation and analysis

Cultures were grown to OD_{600} = 0.5 in 100 mL of YPD medium at 30 °C. Cycloheximide was added to a final concentration of 100 μg/mL just before harvesting. Cells were washed with ice-cold buffer A (100 mM KCl, 20 mM HEPES, pH 7.4, 2 mM magnesium acetate, 50 μg/mL cycloheximide) and resuspended in 500 μL of the same buffer. An equal volume of acid-washed cold glass beads (400 μm in diameter; Sigma Chemical Co.) was added, and the suspension was vortexed eight times for 30 s punctuated with 1 min of cooling on ice. Cell extracts were clarified by centrifugation, and 10 A_{260} units of cell lysate was loaded onto 10-mL linear 10–50% sucrose gradient in buffer (70 mM NH_4Cl, 10 mM Tris, pH 7.4, 4 mM magnesium acetate) and centrifuged at 40,000 rpm in a Beckman SW41 rotor for 2.5 h. Sucrose gradients were analyzed by continuous monitoring at A_{254} with a UV detector (ISCO UA-6).

Preparation of a yeast cell-free system for translation in vitro

Cells from wild-type or mutant strains of *S. cerevisiae* were grown to OD_{600} = 0.9 in YPD. S30 extracts were prepared as described (Hussain & Leibowitz, 1986; Synetos & Coutsogeorgopoulos, 1987; Leibowitz et al., 1991) with some modifications. These include the exposure of the S30 extracts to 0.1 mM of the antibiotic puromycin in the presence of 0.1 mM GTP at 30 °C for 20 min to release the nascent polypeptide chains. The puromycin-treated crude S30 extract was then applied to a Sephadex G-10 column. Excluded fractions with the highest A_{260} were pooled and processed. They contained about 50 A_{260} ribosomes/mL and 6–10 mg protein/mL.

To obtain ribosomes and soluble protein factors, the S30 extract was centrifuged for 3 h at 125,000 × *g*. The ribosome pellet was resuspended in buffer (30 mM HEPES-KOH, pH 7.4, 100 mM potassium acetate, 2 mM magnesium acetate, 2 mM DTT) and clarified by centrifugation at 10,000 × *g* for 10 min to remove any insoluble material. Soluble protein factors were obtained by 0–70% ammonium sulphate precipitation of the S125 supernatant followed by dialysis in the same buffer.

Translation of poly(U) templates in vitro

Translation of poly(U) templates was carried out as described recently (Synetos et al., 1996) using, per 0.1 mL, 25 μg deacylated yeast tRNA, 0.3 nmol [^{3}H]-phenylalanine, and 0.23 nmol L-leucine (for the incorporation of phenylalanine experiments), or 0.3 nmol [^{3}H]-leucine and 0.22 nmol L-phenylalanine (for the misincorporation of leucine experiments). Translation mixtures also contained 1.5 A_{260} units of ribosomes, 25 μg poly(U) and 100 μg of soluble protein factors. The accuracy of translation is expressed as the error frequency, that is, the ratio of the incorporated [^{3}H]-leucine to the combined incorporation of [^{3}H]-leucine plus [^{3}H]-phenylalanine. It represents the number of errors per translated codon.

For time course measurements of polyphenylalanine synthesis, [^{3}H]-Phe-tRNA was prepared by aminoacylation of a mixture of yeast tRNAs with 10 pmol [^{3}H]Phe (250,000

cpm/A_{260} unit), essentially as described previously for the preparation of [^{3}H]Phe-tRNA from *E. coli* (Synetos & Coutsogeorgopoulos, 1987). Reaction mixtures were incubated at 30 °C for the appropriate time intervals and the reaction was stopped by adding an equal volume of 1 N KOH.

Binding of tRNA to the P- and A-sites of the ribosome

The P-site binding was carried out in 0.1 mL of a binding buffer (80 mM Tris-HCl, pH 7.4, 160 mM NH_4Cl, 11 mM $Mg(CH_3COO)_2$, 6 mM β-mercaptoethanol, 0.4 mM GTP, 2 mM spermidine) containing 2.5 A_{260} units of ribosomes, 40 μg poly(U), and 1.3 A_{260} units of yeast Ac-[^{3}H]Phe-tRNA^{Phe}. Reaction mixtures were incubated at 30 °C for 16 min and reaction was stopped by dilution with cold binding buffer. The formed {N-Ac-[^{3}H]Phe-tRNA^{Phe}•80S•poly(U)} complex was immobilized on cellulose nitrate filters and washed three times with the same buffer. The amount of radioactivity retained on the filter was determined by scintillation counting.

Binding of tRNA to the A-site of the ribosome was measured as previously described (Lill et al., 1984). Briefly, the P-site was occupied first with an excess of yeast total tRNA, containing tRNA^{Phe} at a molar ratio of 4:1 over the ribosome concentration. In these conditions, the P-sites of the wild-type and *rdn*-mutant ribosomes were completely filled with tRNA^{Phe}, scored as inability of Ac-Phe-tRNA^{Phe} to bind to the P-site of the ribosome and form Ac-Phe-puromycin product in a titration assay (data not shown). Thus, the occupation of the P-sites with tRNA^{Phe} was performed in 0.1 mL of binding buffer containing 15 mM $Mg(CH_3COO)_2$ by adding 40 μg poly(U), 2.5 A_{260} units of ribosomes, 0.1 mg of soluble protein factors, and tRNA^{Phe} at a molar ratio of 4:1 to ribosomes. The reaction mixtures were incubated at 30 °C for 30 min to fill all P-sites, after which 1.3 A_{260} units of yeast [^{3}H]Phe-tRNA^{Phe} were added. Following reincubation at 30 °C for 10 min to form [^{3}H]Phe-tRNA^{Phe}•80S•poly(U) complex, the reaction was stopped by dilution with cold binding buffer and the complex was immobilized to cellulose nitrate filter disks. The radioactivity measured represents Phe-tRNA^{Phe} binding to the A-site of the ribosome.

Ac-[^{3}H]Phe-tRNA^{Phe} was prepared from a mixture of yeast tRNAs according to a method described previously (Synetos & Coutsogeorgopoulos, 1987). By using this method, Ac-[^{3}H]Phe- tRNA^{Phe} was charged with 14.9 pmol of [^{3}H]Phe (170,000 cpm total)/A_{260} unit. The puromycin reaction in solution was carried out essentially as described previously for *E. coli* ribosomes (Coutsogeorgopoulos et al., 1975).

ACKNOWLEDGMENTS

We thank Dmitri Pestov, Zaklina Strezoska, and Tanel Tenson for helpful comments on the manuscript and Mary Nelson for technical assistance. We are grateful to Yury Chernoff for yeast strains. This work was supported by National Institutes of Health Grants GM 51412, GM 53762, and TW00870.

Received March 17, 2000; returned for revision April 12, 2000; revised manuscript received May 12, 2000

REFERENCES

Arkov AL, Freistroffer DV, Ehrenberg M, Murgola EJ. 1998. Mutations in RNAs of both ribosomal subunits cause defects in translation termination. *EMBO J 17*:1507–1514.

Boeke JD, LaCroute F, Fink GR. 1984. A positive selection for mutants lacking orotidine-5′-phosphate decarboxylase activity in yeast: 5-fluoro-orotic acid resistance. *Mol Gen Genet 197*: 345–346.

Cate JH, Yusupov MM, Yusupova GZ, Earnest TN, Noller HF. 1999. X-ray crystal structures of 70S ribosome functional complexes. *Science 285*:2095–2104.

Chernoff YO, Newnam GP, Liebman SW. 1996. The translational function of nucleotide C1054 in the small subunit rRNA is conserved throughout evolution: Genetic evidence in yeast. *Proc Natl Acad Sci USA 93*:2517–2522.

Chernoff YO, Vincent A, Liebman SW. 1994. Mutations in eukaryotic 18S ribosomal RNA affect translational fidelity and resistance to aminoglycoside antibiotics. *EMBO J 13*:906–913.

Clemons WM Jr, May JL, Wimberly BT, McCutcheon JP, Capel MS, Ramakrishnan V. 1999. Structure of a bacterial 30S ribosomal subunit at 5.5 Å resolution. *Nature 400*:833–840.

Coutsogeorgopoulos C, Miller JT, Hann DM. 1975. Inhibitors of protein synthesis V. Irreversible interaction of antibiotics with an initiation complex. *Nucleic Acids Res 2*:1053–1072.

Fourmy D, Yoshizawa S, Puglisi JD. 1998. Paromomycin binding induces a local conformational change in the A-site of 16 S rRNA. *J Mol Biol 277*:333–345.

Gabashvili IS, Agrawal RK, Grassucci R, Squires CL, Dahlberg AE, Frank J. 1999. Major rearrangements in the 70S ribosomal 3D structure caused by a conformational switch in 16S ribosomal RNA. *EMBO J 18*:6501–6507.

Grant P, Sanchez L, Jimenez A. 1974. Cryptopleurine resistance: Genetic locus for a 40S ribosomal component in *Saccharomyces cerevisiae*. *J Bacteriol 120*:1308–1314.

Gutell RR, Larsen N, Woese CR. 1994. Lessons from an evolving rRNA: 16S and 23S rRNA structures from a comparative perspective. *Microbiol Rev 58*:10–26.

Hinnebusch AG, Liebman SW. 1991. Protein synthesis and translational control in *Saccharomyces cerevisiae*. In: Broach JR, Pringle JR, Jones JW, eds. *The molecular and cellular biology of the yeast Saccharomyces*. Cold Spring Harbor, New York: Cold Spring Harbor Laboratory Press. pp 627–735.

Hopfield JJ. 1974. Kinetic proofreading: A new mechanism for reducing errors in biosynthetic processes requiring high specificity. *Proc Natl Acad Sci USA 71*:4135–4139.

Hussain I, Leibowitz MJ. 1986. Translation of homologous and heterologous messenger RNAs in a yeast cell-free system. *Gene 46*:13–23.

Ito H, Fukuda Y, Murata K, Kimura A. 1983. Transformation of intact yeast cells treated with alkali cations. *J Bacteriol 153*:163–168.

Ito W, Ishiguro H, Kurosawa Y. 1991. A general method for introducing a series of mutations into cloned DNA using the polymerase chain reaction. *Gene 102*:67–70.

Kawakami K, Nakamura Y. 1990. Autogenous suppression of an opal mutation in the gene encoding peptide chain release factor 2. *Proc Natl Acad Sci USA 87*:8432–8436.

Kraal B, Zeef LA, Mesters JR, Boon K, Vorstenbosch EL, Bosch L, Anborgh PH, Parmeggiani A, Hilgenfeld R. 1995. Antibiotic resistance mechanisms of mutant EF-Tu species in *Escherichia coli*. *Biochem Cell Biol 73*:1167–1177.

Kurland CG. 1992. Translational accuracy and the fitness of bacteria. *Annu Rev Genet 26*:29–50.

Leibowitz MJ, Barbone FP, Georgopoulos DE. 1991. In vitro protein synthesis. *Methods Enzymol 194*:536–545.

Liebman SW, Chernoff YO, Liu R. 1995. The accuracy center of a eukaryotic ribosome. *Biochem Cell Biol 73*:1141–1149.

Lill R, Robertson JM, Wintermeyer W. 1984. tRNA binding sites of ribosomes from *Escherichia coli*. *Biochemistry 23*:6710–6717.

Liu R, Liebman SW. 1996. A translational fidelity mutation in the universally conserved sarcin/ricin domain of 25S yeast ribosomal RNA. *RNA 2*:254–263.

Lodmell JS, Dahlberg AE. 1997. A conformational switch in *Escherichia coli* 16S ribosomal RNA during decoding of messenger RNA. *Science 277*:1262–1267.

Lodmell JS, Gutell RR, Dahlberg AE. 1995. Genetic and comparative analyses reveal an alternative secondary structure in the region of nt 912 of *Escherichia coli* 16S rRNA. *Proc Natl Acad Sci USA 92*:10555–10559.

Mathews DH, Sabina J, Zuker M, Turner DH. 1999. Expanded sequence dependence of thermodynamic parameters improves prediction of RNA secondary structure. *J Mol Biol 288*:911–940.

Merryman C, Moazed D, McWhirter J, Noller HF. 1999. Nucleotides in 16S rRNA protected by the association of 30S and 50S ribosomal subunits. *J Mol Biol 285*:97–105.

Moazed D, Noller HF. 1986. Transfer RNA shields specific nucleotides in 16S ribosomal RNA from attack by chemical probes. *Cell 47*:985–994.

Moazed D, Noller HF. 1987. Interaction of antibiotics with functional sites in 16S ribosomal RNA. *Nature 327*:389–394.

Mueller F, Brimacombe R. 1997. A new model for the three-dimensional folding of *Escherichia coli* 16 S ribosomal RNA. I. Fitting the RNA to a 3D electron microscopic map at 20 Å. *J Mol Biol 271*:524–544.

Mugnier P, Tuite MF. 1999. Translation termination and its regulation in eukaryotes: Recent insights provided by studies in yeast. *Biochemistry* (Mosc) *64*:1360–1366.

O'Connor M, Goringer HU, Dahlberg AE. 1992. A ribosomal ambiguity mutation in the 530 loop of *E. coli* 16S rRNA. *Nucleic Acids Res 20*:4221–4227.

O'Connor M, Thomas CL, Zimmermann RA, Dahlberg AE. 1997. Decoding fidelity at the ribosomal A and P sites: Influence of mutations in three different regions of the decoding domain in 16S rRNA. *Nucleic Acids Res 25*:1185–1193.

Pagel FT, Zhao SQ, Hijazi KA, Murgola EJ. 1997. Phenotypic heterogeneity of mutational changes at a conserved nucleotide in 16 S ribosomal RNA. *J Mol Biol 267*:1113–1123.

Palmer E, Wilhelm JM, Sherman F. 1979. Phenotypic suppression of nonsense mutants in yeast by aminoglycoside antibiotics. *Nature 277*:148–150.

Pape T, Wintermeyer W, Rodnina M. 1999. Induced fit in initial selection and proofreading of aminoacyl-tRNA on the ribosome. *EMBO J 18*:3800–3807.

Parent SA, Fenimore CM, Bostian KA. 1985. Vector systems for the expression, analysis and cloning of DNA sequences in *S. cerevisiae*. *Yeast 1*:83–138.

Puglisi JD, Blanchard SC, Dahlquist KD, Eason RG, Fourmy D, Lynch SR, Recht MI, Yoshizava S. 2000. Aminoglycoside antibiotics and decoding. In: Garrett RA, Douthwaite SR, Liljas A, Matheson AT, Moore PB, Noller HF, eds. *The ribosome: Structure, function, antibiotics, and cellular interactions*. Washington, D.C.: ASM Press. pp 419–429.

Rose MD, Winston WF, Hieter P. 1990. *Methods in yeast genetics: A laboratory course manual.* Cold Spring Harbor, New York: Cold Spring Harbor Laboratory Press.

Ruusala T, Ehrenberg M, Kurland CG. 1982. Is there proofreading during polypeptide synthesis? *EMBO J 1*:741–745.

Sambrook J, Fritsch EF, Maniatis T. 1989. *Molecular cloning: A laboratory manual.* Cold Spring Harbor, New York: Cold Spring Harbor Laboratory Press.

Song H, Mugnier P, Das AK, Webb HM, Evans DR, Tuite MF, Hemmings BA, Barford D. 2000. The crystal structure of human eukaryotic release factor eRF1: Mechanism of stop codon recognition and peptidyl–tRNA hydrolysis. *Cell 100*:311–321.

Stern S, Powers T, Changchien LM, Noller HF. 1989. RNA–protein interactions in 30S ribosomal subunits: Folding and function of 16S rRNA. *Science 244*:783–790.

Stern S, Wilson RC, Noller HF. 1986. Localization of the binding site for protein S4 on 16 S ribosomal RNA by chemical and enzymatic probing and primer extension. *J Mol Biol 192*:101–110.

Synetos D, Coutsogeorgopoulos C. 1987. Studies on the catalytic rate constant of ribosomal peptidyltransferase. *Biochim Biophys Acta 923*:275–285.

Synetos D, Frantziou CP, Alksne LE. 1996. Mutations in yeast ribosomal proteins S28 and S4 affect the accuracy of translation and alter the sensitivity of the ribosomes to paromomycin. *Biochim Biophys Acta 1309*:156–166.

Thompson RC, Dix DB, Karim AM. 1986. The reaction of ribosomes with elongation factor Tu·GTP complexes. Aminoacyl–tRNA-independent reactions in the elongation cycle determine the accuracy of protein synthesis. *J Biol Chem 261*:4868–4874.

VanLoock MS, Easterwood TR, Harvey SC. 1999. Major groove binding of the tRNA/mRNA complex to the 16 S ribosomal RNA decoding site. *J Mol Biol 285*:2069–2078.

Vijgenboom E, Vink T, Kraal B, Bosch L. 1985. Mutants of the elongation factor EF-Tu, a new class of nonsense suppressors. *EMBO J 4*:1049–1052.

Wilson KS, Noller HF. 1998. Molecular movement inside the translational engine. *Cell 92*:337–349.

Yoshizawa S, Fourmy D, Puglisi JD. 1999. Recognition of the codon-anticodon helix by ribosomal RNA. *Science 285*:1722–1725.

Zuker M, Jacobson AB. 1998. Using reliability information to annotate RNA secondary structures. *RNA 4*:669–679.